Structural properties of the synchronized cluster on complex networks

Yup Kim,* Yongjin Ko, and Soon-Hyung Yook†
Department of Physics and Research Institute for Basic Sciences, Kyung Hee University, Seoul 130-701, Korea
(Received 13 October 2008; revised manuscript received 22 June 2009; published 29 January 2010)

We investigate how the largest synchronized connected component (LSCC) is formed and evolves to achieve a global synchronization on complex networks using Kuramoto model. In this study we use two different networks, Erdösi-Rényi network and Barabási-Albert network. From the finite-size scaling analysis, we find that the scaling exponents for the percolation order parameter and mean cluster size on both networks agree with the mean-field percolation theory, $\beta=\gamma=1$. We also find that the finite-size scaling exponent, $\bar{\nu}$, also agrees with the mean-field percolation result, $\bar{\nu}=3$. Moreover, we also show that the cluster size distributions are identical with the mean-field percolation distribution on both networks. Combining with the analysis for the merging clusters, we directly show that the LSCC on both networks evolves by merging clusters of various sizes.

DOI: 10.1103/PhysRevE.81.011139 PACS number(s): 64.60.aq, 05.45.Xt, 64.60.ah, 89.75.Hc

Recent studies have revealed that the topological properties of interactions in various systems are well described by complex networks [1]. These complex networks share some common properties such as small-world phenomena [2]. The relationship between the topological properties of interaction networks and the various dynamical properties, such as the emergence of collective behavior, has been one of the main research topics in complex network studies [3,4].

The emergence of collective synchronized phenomena is easily found in many diverse branches of science such as physics, biology, computer science, chemistry, and sociology [5,6]. Among the many theoretical models to understand the collective synchronized phenomena, Kuramoto proposed a simple model of coupled phase oscillators [5]. In the original Kuramoto model (KM) each oscillator is coupled with all other oscillators. This global coupling causes a synchronization transition. For locally coupled oscillators in d-dimension, $d=2$ is generally accepted as the lower critical dimension for macroscopic entrainment [7]. For $2<d\leq 4$, KM shows a frequency entrainment without phase ordering [8]. For $d>4$ merging various clusters plays a key role for the synchronization transition, and the transition belongs to the mean-field universality class [8].

On complex networks, the structure of interaction between each unit affects the synchronization transition of KM. Many studies have shown that the small-world feature increases the stability of the synchronized state of KM [9,10]. However, the synchronization dynamics on complex networks has not been fully understood. For example, on scale-free (SF) networks in which the degree distribution satisfies a power law, $P(k)\sim k^{-\lambda}$, the heterogeneity in degree is known to suppresses the global synchronizability based on the linear stability analysis [11]. In contrast to the linear stability analysis, mean-field type approaches, such as time averaged approximation and frequency distribution approximation, predict that the system is always in the synchronized state for $\lambda<3$ and show a phase transition when $\lambda>3$ [12–14]. For $\lambda=3$ the numerical simulation [14,15] predicts that KM undergoes a phase transition. Since the synchronization transition is known to be caused by the formation of the synchronized cluster [8,13], we study the structural properties of synchronized clusters of KM in this paper to understand how the globally synchronized states are achieved.

Recently, the physical route to a global synchronization was studied on random networks (RNs) and SF networks with $\lambda=3$ [16]. Based on the analysis of the size of the largest synchronized connected component (LSCC) and the number of synchronized connected components, they suggested that many different clusters of synchronized oscillators merge together to form LSCC in Erdös-Rényi (ER) network as increasing the coupling coefficient [16]. In contrast to ER network, they claimed that LSCC in SF networks incorporates other oscillators one-by-one as the coupling coefficient increases [16]. In this paper based on the analysis of the percolation transition [17] and direct measurement of the merged cluster size distribution on complex networks, we also show that the physical route to a global synchronization are identical when $\lambda\geq 3$.

The KM consists of N locally coupled phase oscillators. The phase of oscillator at node i, θ_i, evolves in time according to [5]

$$\frac{d\theta_i}{dt}=\omega_i+J\sum_{j=1}^{N}A_{ij}\sin(\theta_j-\theta_i)\quad(i=1,2,\ldots,N),\qquad(1)$$

where ω_i is the natural frequency of oscillator i and A_{ij} represents the adjacency matrix ($A_{ij}=1$ if two nodes i and j are connected and 0 otherwise). We solve Eq. (1) using the fourth-order Runge-Kutta method with uniform distribution of ω_i in the interval $[-1/2,1/2]$ [16,18]. To construct the synchronized cluster, we use a coherence parameter [16]

$$\Delta=\frac{1}{2L}\sum_{i=1}^{N}\sum_{j=1}^{N}A_{ij}\left|\lim_{T\to\infty}\frac{1}{T}\int_{t_r}^{t_r+T}e^{i[\theta_i(t)-\theta_j(t)]}dt\right|,\qquad(2)$$

where L is the number of edges in the network. Equation (2) represents the fraction of all possible edges that are synchronized for time interval $[t_r,t_r+T]$ after the system is relaxed to

*ykim@khu.ac.kr
†syook@khu.ac.kr

the stable state. From Eq. (2) we define the coherence matrix as

$$D_{ij} = A_{ij} \left| \lim_{T\to\infty} \frac{1}{T} \int_{t_r}^{t_r+T} e^{i[\theta_i(t)-\theta_j(t)]} dt \right| . \quad (3)$$

Here D_{ij} represents the contribution of a pair oscillators i and j into Eq. (2). To filter out the matrix we use a threshold c^* at which the fraction of synchronized pair equals Δ. In this way, if $D_{ij} > c^*$ then two connected oscillators i and j are considered to be synchronized and belong to the same cluster [16]. The choice of c^* does not affect the main results. This changes only the critical point, J_c for the percolation transition.

In the percolation theory on complex networks [17,19], the order parameter, P_∞, is defined by the probability that a node belongs to a giant cluster. For a given occupation probability p, P_∞ satisfies a power-law scaling, $P_\infty \sim (p-p_c)^\beta$, near the percolation threshold p_c. Similarly, the mean cluster size follows a power law, $S \sim |p-p_c|^{-\gamma}$. The mean-field exponents are $\beta=1$ and $\gamma=1$ [17]. The order parameter in the synchronization transition is closely related to the size of LSCC at synchronization critical point J_c [13]. Thus, in order to study the structural properties of synchronized cluster as a function of J, we use the following ansatz for P_∞ and S [19]

$$P_\infty(J) \sim (J-J_c)^\beta, \quad \text{and} \quad S(J) \sim |J-J_c|^{-\gamma}. \quad (4)$$

For finite size of networks with N nodes, P_∞ is assumed to satisfy the finite-size scaling as

$$P_\infty(J,N) = N^{-\beta/\bar{\nu}} f[(J-J_c)N^{1/\bar{\nu}}]. \quad (5)$$

Here, $\bar{\nu}$ is the finite-size scaling exponent and the scaling function, $f(x)$, satisfies $f(x) \sim x^\beta$ for $x \gg 1$ and $f(x)=$const for $x \ll 1$. Similarly, $S(J,N)$ satisfies a scaling ansatz

$$S(J,N) = N^{\gamma/\bar{\nu}} g(|J-J_c|N^{1/\bar{\nu}}), \quad (6)$$

where the scaling function $g(x)$ also has the asymptotic form $g(x) \sim x^{-\gamma}$ for $x \gg 1$ and $g(x)=$const for $x \ll 1$. According to the finite-size scaling ansatz, the value of J at which $S(J,N)$ has maximum, $S_{\max}(J_{\max},N)$, approaches J_c as [19]

$$J_{\max}(N) = J_c + aN^{-1/\bar{\nu}}, \quad (7)$$

where a is a constant.

In order to study the effects of the underlying topology we consider two networks: (1) ER network [20] and (2) Barabási-Albert (BA) network [21,22]. Each data are averaged over 1000 network realizations. The average degree of network is fixed to be $\langle k \rangle = 6$. In Figs. 1(a) and 1(b) we display $J_{\max}(N)$ for various N on both ER and BA networks. From the best fit of Eq. (7) to the data we obtain $J_c = 0.033 \pm 0.001$ and $\bar{\nu} = 3.1 \pm 0.1$ on ER networks and $J_c = 0.017 \pm 0.001$ and $\bar{\nu} = 3.1 \pm 0.1$ on BA networks. There is a little subtlety in the value of $\bar{\nu}$. Based on the droplet-excitation argument, $\bar{\nu}$ is conjectured as the product of the mean-field correlation length exponent, ν_{MF} and the upper critical dimension, d_u, i.e., $\bar{\nu} = d_u \nu_{MF}$ [23]. This conjecture yields $\bar{\nu}=3$ ($\nu_{MF}=1/2$ and $d_u=6$). The numerically estimated values of $\bar{\nu}$ on both networks are very close to that of the mean-field percolation theory.

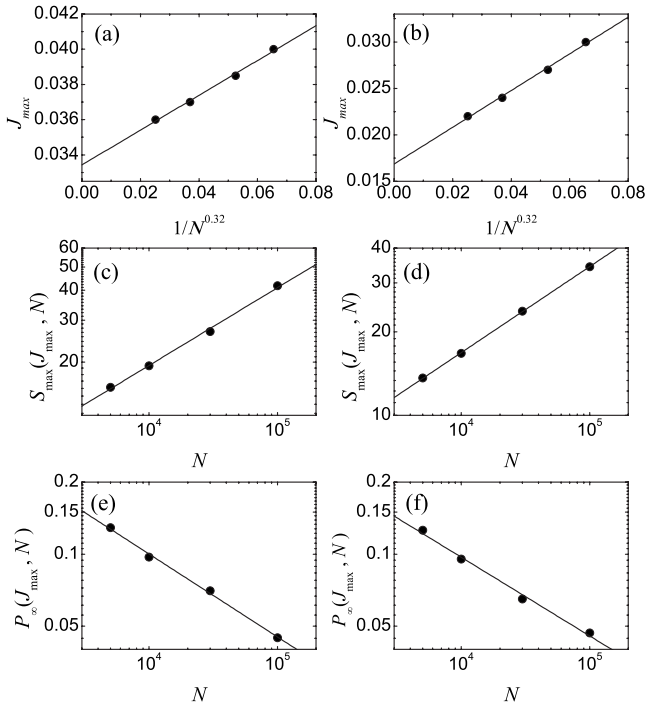

FIG. 1. Plot of $J_{\max}(N)$ in (a) ER networks and (b) BA networks. The intercept with $J_{\max}$-axis corresponds to J_c. Plot of $S_{\max}(J_{\max},N)$ against N on (c) ER networks and (d) BA networks. The solid lines represent the relation (8). (e) and (f) show $P_\infty(J_{\max},N)$ on ER and BA networks, respectively. The solid lines stand for Eq. (9).

Equation (6) indicates that $S_{\max}(J_{\max},N)$ grows as

$$S_{\max}(J_{\max},N) \sim N^{\gamma/\bar{\nu}}. \quad (8)$$

In Figs. 1(c) and 1(d) we show $S_{\max}(J_{\max},N)$ on ER networks and BA networks, respectively. From the least square fit of Eq. (8) to the data we obtain $\gamma/\bar{\nu} = 0.32 \pm 0.01$ on ER networks and $\gamma/\bar{\nu} = 0.31 \pm 0.01$ on BA networks. Using the estimated $\bar{\nu}$ we obtain $\gamma = 0.99 \pm 0.04$ for ER networks and $\gamma = 0.96 \pm 0.04$ for BA networks. These values of γ are consistent with the mean-field value $\gamma=1$ within the estimated errors. Similarly, from Eq. (5) we obtain the relation,

$$P_\infty(J_{\max},N) \sim N^{-\beta/\bar{\nu}}. \quad (9)$$

In Figs. 1(e) and 1(d) we display the measured $P_\infty(J_{\max},N)$ for various N. Using Eq. (9) we find $\beta/\bar{\nu} = 0.34 \pm 0.02$ on ER networks and $\beta/\bar{\nu} = 0.33 \pm 0.02$ on BA networks. Thus, we obtain $\beta = 1.05 \pm 0.07$ and $\beta = 1.02 \pm 0.07$ for ER networks and BA networks, respectively. The obtained βs also agree with the mean-field value $\beta=1$ within the estimated error. These critical exponents on both networks show that the formation of the synchronized cluster belongs to the mean-field percolation universality class, regardless of the underlying network topology.

In Figs. 2(a) and 2(b) we show the scaling plot of $P_\infty(J,N)$ in ER networks and BA networks, respectively. The data in Figs. 2(a) and 2(b) show that $P_\infty(J,N)$ of the synchronized cluster satisfy the relation (5) very well with the obtained J_c, $\bar{\nu}$ and β from the data in Fig. 1. We also show a scaling plot of $S(J,N)$ for both networks in Figs. 2(c) and

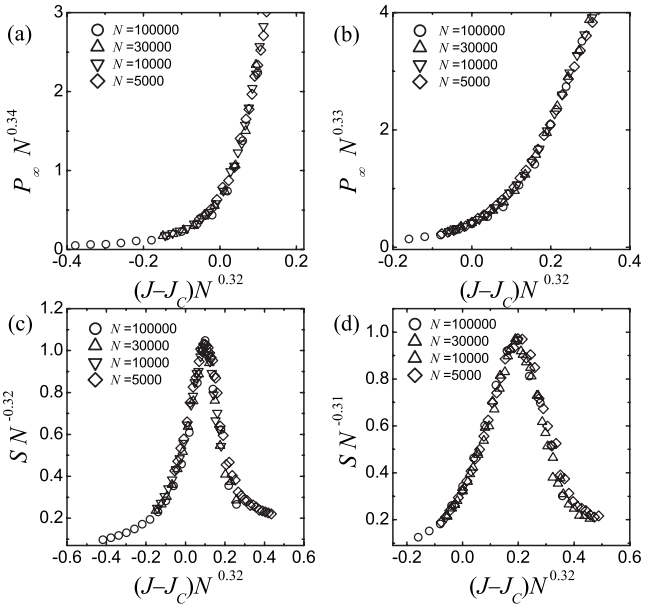

FIG. 2. Scaling plot of P_∞ on (a) ER networks and (b) BA networks. Scaling plot of S on (c) ER networks (d) BA networks.

2(d). Using the obtained J_c, β and $\bar{\nu}$, we also verify that $S(J,N)$ collapses into a single curve which satisfies the universal function (6). Interestingly, the results show that the percolation transition of the synchronized cluster is not affected by the underlying topology when there is the synchronization transition ($\lambda \geq 3$).

In order to investigate how LSCC is formed, we first measure the cluster number, $n_s(J)=N_s(J)/N$ [17], for various values of J. Here, $N_s(J)$ is the number of clusters of size s when the coupling strength is J. In our measurement, we include LSCC in n_s. As shown in Fig. 3(a), $n_s(J)$ satisfies the power law;

$$n_s \sim s^{-\tau}, \tag{10}$$

when $J=J_{\max}(N)$. From the data in Fig. 3(a) we obtain $\tau=2.7\pm0.3$ for both ER and BA networks when $J=J_{\max}(N)$. The obtained τ at $J=J_{\max}(N)$ ($\simeq J_c$) also agrees well with the mean-field value $\tau=5/2$ within the estimated error on both networks. For $J>J_c$, n_s around $s\sim10^4$ in Fig. 3(b) clearly shows the formation of LSCC on both networks. The value

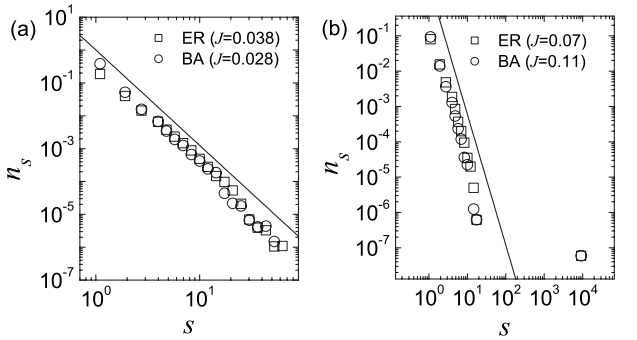

FIG. 3. Plot of n_s at (a) $J\simeq J_{\max}(N)$ ($\approx J_c$) and (b) $J>J_c$ when $N=10\,000$. The solid lines represent (a) $\tau=2.7$ and (b) $\tau=3.7$.

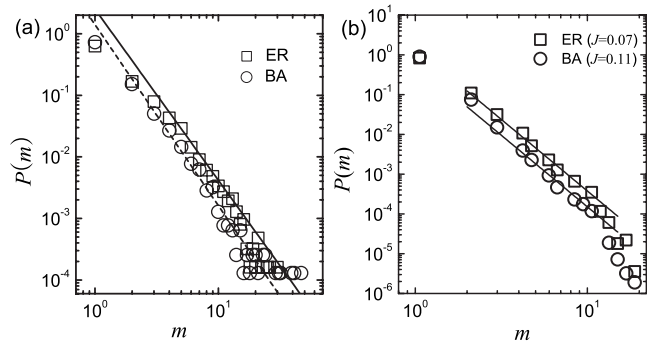

FIG. 4. (a) Plot of $P(m)$ for $J=0.06$. The lines represent the relation $P(m)\sim m^{-\delta}$ with $\delta=2.8$ for ER network (solid line) and $\delta=2.9$ for SF network (dashed line). (b) Plot of $P(m)$ for $N_{\mathrm{LSCC}}\simeq0.86N$. Solid lines denote $\delta=3.6$.

of τ increases as J increases when $J>J_c$. The obtained τ for both networks are almost the same. For example, Fig. 3(b) shows the n_s when the size of LSCC is approximately 80% of N. From the best fit with Eq. (10) to the data except for the data of LSCC, we obtain $\tau=3.7\pm0.1$ for both networks.

From the measurement of the size of LSCC and the number of synchronized connected components for various values of J, Gómez-Gardeñes *et al.* [16] claimed that the route to achieve a global synchronization on BA network is different from that on ER networks when $J>J_c$. But the analysis provided by Gómez-Gardeñes *et al.* is rather indirect. For the complete understanding on the physical route to the globally synchronized state, we directly measure the size distribution of the merged clusters into LSCC. For this purpose, we use the simulated annealing method [24]. Starting from $J=0.01$ the systems is relaxed to reach a stationary state in which the synchronization order parameter, $r=(1/N)|\Sigma_{j=1}^{N}\exp(i\theta_j)|$, remains constant. Then, increase J by δJ (=0.01). The final state for J of the simulation is used as the initial state for $J+\delta J$. The system is again relaxed to reach a stationary state. By comparing between the two successive stationary states, we directly measure the size distribution of the merging cluster, $P(m)$. As shown in Fig. 4, the value of $P(m)$ are almost identical on both networks when $J>J_c$. Moreover, the maximum value of merging cluster, $m_{\max}$, are the almost same on both networks when $N_{\mathrm{LSCC}}>N/2$ (see Fig. 4). The value of $m_{\max}$ are very small compared to N_{LSCC}. This is natural consequence of percolation transition. As shown in Fig. 3(b), most of the nodes belong to the LSCC and the size of non-LSCC cluster is very small compared to that of LSCC when $J>J_c$ for both networks. Therefore, only small finite clusters can be merged into LSCC. The value of $P(m)$ in Fig. 4 clearly shows that the LSCC evolves by merging these finite small clusters on both networks.

If we assume the power-law distribution, $P(m)\sim m^{-\delta}$, then we obtain $\delta=2.8\pm0.3$ for ER network and $\delta=2.9\pm0.3$ for BA networks when the coupling coefficient changes from $J=0.05$ to $J=0.06$ [see Fig. 4(a)]. This value of J ensures that the size of LSCC exceeds $N/2$ in both ER and BA networks. Since the size of the LSCC, N_{LSCC}, on ER network is different from that on BA network for the same J [16], we also measure $P(m)$ when N_{LSCC}s on both networks are the same ($N_{\mathrm{LSCC}}\simeq0.86N$). This value of N_{LSCC} corre-

sponds to $J=0.07$ for ER network and $J=0.11$ for BA network. As shown in Fig. 4(b), we obtain $\delta=3.6\pm0.2$ on both ER and BA networks for $m<10$. When $m>10$, $P(m)$ abruptly decays on both networks. From our measurements we find that $P(m)$ on both networks satisfies $P(m)\sim m^{-\delta}$ with the same δ when $N/2<N_{\mathrm{LSCC}}<N$. In summary, the straight lines in Fig. 4 just imply that if we assume the power law for $P(m)$ then we can also find the same exponents on both networks. But the more important fact is that the difference in $P(m)$ on both networks are negligible. Combining the results shown in Figs. 1–4, we conclude that the underlying mechanisms to form a globally synchronized cluster on both networks are identical, in contrast to the results of Gómez-Gardeñes *et al.* [16].

This work was supported by the Korea Science and Engineering Foundation (KOSEF) grant funded by the Korea government (MEST) (Grant No. 2009-0052659) and by the Korea Research Foundation grant funded by the Korean Government (MOEHRD, Basic Research Promotion Fund) (Grants No. KRF-2007-313-C00279 and No. KRF-2008-331-C00109).

[1] R. Albert and A.-L. Barabási, Rev. Mod. Phys. **74**, 47 (2002).
[2] D. J. Watts and S. H. Strogatz, Nature (London) **393**, 440 (1998).
[3] S. Lee, S.-H. Yook, and Y. Kim, Phys. Rev. E **74**, 046118 (2006).
[4] D. Garlaschelli, A. Capocci, and G. Caldarelli, Nat. Phys. **3**, 813 (2007).
[5] Y. Kuramoto, in *Proceedings of the International Symposium on Mathematical Problems in Theoretical Physics*, edited by H. Araki (Springer-Verlag, Berlin, 1975).
[6] A. S. Pikovsky, M. Rosenblum, and J. Kurths, *Synchronization: A Universal Concept in Nonlinear Science* (Cambridge University Press, Cambridge, England, 2001).
[7] S. H. Strogatz and R. E. Mirollo, Physica D **31**, 143 (1988).
[8] H. Hong, H. Chaté, H. Park, and L.-H. Tang, Phys. Rev. Lett. **99**, 184101 (2007).
[9] M. Barahona and L. M. Pecora, Phys. Rev. Lett. **89**, 054101 (2002).
[10] H. Hong, M. Y. Choi, and B. J. Kim, Phys. Rev. E **65**, 026139 (2002).
[11] T. Nishikawa, A. E. Motter, Y.-C. Lai, and F. C. Hoppensteadt, Phys. Rev. Lett. **91**, 014101 (2003).
[12] D.-S. Lee, Phys. Rev. E **72**, 026208 (2005).
[13] E. Oh, D.-S. Lee, B. Kahng, and D. Kim, Phys. Rev. E **75**, 011104 (2007).
[14] J. G. Restrepo, E. Ott, and B. R. Hunt, Phys. Rev. E **71**, 036151 (2005); Chaos **16**, 015107 (2006).
[15] Y. Moreno and A. F. Pacheco, Europhys. Lett. **68**, 603 (2004).
[16] J. Gómez-Gardeñes, Y. Moreno, and A. Arenas, Phys. Rev. Lett. **98**, 034101 (2007); Phys. Rev. E **75**, 066106 (2007).
[17] D. Stauffer and A. Aharony, *Introduction to Percolation Theory* (Taylor & Francis, London, 1994).
[18] In the percolating phase the macroscopic spanning (synchronized) cluster should exist. Therefore, the variance of ω_i should not diverge: see, for example, A. Arenas, A. Díaz-Guilera, J. Kurths, Y. Moreno, and C. Zhou, Phys. Rep. **469**, 93 (2008).
[19] J. D. Noh, Phys. Rev. E **76**, 026116 (2007).
[20] P. Erdös and P. Rényi, Publ. Math. (Debrecen) **6**, 290 (1959).
[21] A.-L. Barabási and R. Albert, Science **286**, 509 (1999).
[22] Since the results on SF networks with $\lambda=3$ and ER networks (which corresponds to $\lambda\to\infty$) are coincide, we expect that the properties of percolation transition of KM on SF networks with $\lambda\geq3$ should be the same.
[23] H. Hong, M. Ha, and H. Park, Phys. Rev. Lett. **98**, 258701 (2007).
[24] H. Gould, J. Tobochnik, and W. Christian, *An Introduction to Computer Simulation Methods: Applications to Physical Systems* (Addison-Wesley, New York, 2007).